

# Dosimetry for $^{125}\text{I}$ seed (model 6711) in eye plaques

Sou-Tung Chiu-Tsao

*Department of Radiation Oncology, Henry Ford Hospital, Detroit, Michigan 48202*

Lowell L. Anderson

*Department of Medical Physics, Memorial Sloan Kettering Cancer Center, New York, New York 10021*

Keran O'Brien

*Department of Physics and Astronomy, Northern Arizona University, Flagstaff, Arizona 86011*

Leonard Stabile

*Department of Radiation Medicine, New York Medical College, Valhalla, New York 10595*

John C. Liu

*Department of Biostatistics, Memorial Sloan Kettering Cancer Center, New York, New York 10021*

(Received 30 May 1991; accepted for publication 10 November 1992)

The effect of eye plaque materials (gold backing and silastic seed-carrier insert) on the dose distribution around a single  $^{125}\text{I}$  seed has been measured, using cubic lithium fluoride thermoluminescent dosimeters (TLDs) 1 mm on an edge, in a solid water eye phantom embedded in a solid water head phantom. With an  $^{125}\text{I}$  seed (model 6711) positioned in the center slot of the silastic insert for a 20-mm plaque of the design used in the collaborative ocular melanoma study (COMS), dose was measured at 2-mm intervals along the plaque central axis (the seed's transverse axis) and at various off-axis points, both with and without the COMS gold backing placed over the insert. Monte Carlo calculations (MORSE code) were performed, as well, for these configurations and closely the same geometry but assuming a large natural water phantom. Additional Monte Carlo calculations treated the case, both for 20- and 12-mm gold plaques, where the silastic insert is replaced by natural water. Relative to previous measurements taken in homogeneous medium of the same material (without the eye plaque), the dose reduction found by both Monte Carlo and TLD methods was greater at points farther from the seed along the central axis and, for a given central-axis depth, at larger off-axis distances. Removal of the gold backing from the plaque did not make measurable difference in the dose reduction results (10% at 1 cm).

**Key words:**  $^{125}\text{I}$  seed, eye plaque, thermoluminescent dosimetry, Monte Carlo calculation, dose distributions

## I. INTRODUCTION

$^{125}\text{I}$  plaques have been used increasingly in recent years in the radiation therapy of ocular tumors.<sup>1-5</sup> In 1986, a 5-year randomized trial, the collaborative ocular melanoma study (COMS), was launched by the National Eye Institute in order to compare survival following irradiation with that following enucleation. For choroidal melanomas with apex heights in the range 3.1–8 mm and base diameters between 8 and 16 mm, irradiation is performed with  $^{125}\text{I}$  plaques.<sup>6</sup> In view of the importance of accurate dosimetry to the evaluation of COMS results, we have performed measurements and calculations pertinent to eye plaque treatments using plaques of the COMS design.

The plaques adopted for the COMS were designed by the Mayo Clinic group.<sup>7</sup> Plaque diameters range from 12–20 mm in 2-mm increments. The  $^{125}\text{I}$  seeds are loaded into fixed slots arranged in rings in a silastic seed-carrier insert. A gold backing of the matching radius of curvature and diameter is glued to the silastic insert at the circular rim to form the complete  $^{125}\text{I}$  eye plaque. The silastic seed carrier insert also serves as a spacer, maintaining at least a 1-mm distance between the exterior scleral surface and the seed surface. In a surgical procedure, the plaque is sutured

to the sclera at the tumor base for a treatment that generally lasts from 5–10 days to deliver a total dose of 10 000 cGy to the tumor apex. The dose rate at the apex is in the range 50–125 cGy/h. With the plaque applied at the tumor base, a complete assessment of the dose distribution requires accurate dose data even at very small distances (down to 0.14 cm) from the source centers.

The  $^{125}\text{I}$  source used in our study is the model 6711 seed, in which the radioactive  $^{125}\text{I}$  is adsorbed on the surface of a silver wire contained within the thin titanium capsule. Dose distributions at short distances from 6711  $^{125}\text{I}$  seeds in homogeneous medium have been reported by Chiu-Tsao *et al.*<sup>8</sup> based on thermoluminescent dosimeter (TLD) measurements in solid water phantom<sup>9</sup> and Monte Carlo calculations in natural water. Williamson,<sup>10</sup> also, has reported the results of Monte Carlo dose calculations in this distance range. A comparison of relative dose data from these studies shows agreement within 5%.

The current recommendation<sup>11</sup> of the COMS group is that the dose rate in tissue at 1 cm along the transverse axis of the seed be taken to be  $1.04 \text{ cGy h}^{-1} \text{ U}^{-1}$  ( $1.32 \text{ cGy h}^{-1} \text{ mCi}^{-1}$ ),<sup>12</sup> which is obtained as the product of the exposure rate constant ( $1.14 \text{ R h}^{-1} \text{ U}^{-1}$  or  $1.45 \text{ R h}^{-1} \text{ mCi}^{-1}$ ) and

the  $f$  factor ( $0.91 \text{ cGy R}^{-1}$ ) in tissue. Chiu-Tsao *et al.*<sup>8</sup> have shown that, for model 6711 seed, the transverse axis dose rate at 1-cm distance is  $0.85 \text{ cGy h}^{-1} \text{ U}^{-1}$  ( $1.08 \text{ cGy h}^{-1} \text{ mCi}^{-1}$ ) in water, and  $0.89 \text{ cGy h}^{-1} \text{ U}^{-1}$  ( $1.12 \text{ cGy h}^{-1} \text{ mCi}^{-1}$ ) in tissue, about 16% less than would have been expected by geometrical (inverse square law) attenuation only. These results were obtained as part of work performed under an interstitial brachytherapy contract with the National Cancer Institute, and were corroborated by data from two collaborating institutions (Yale Medical Center and the University of California, San Francisco).<sup>13-15</sup>

However, the effect of the eye plaque itself, i.e., the gold backing and the silastic seed-carrier insert, on the  $^{125}\text{I}$  dose distributions at short distances remains an important issue to be resolved. Weaver measured doses with TLD powder in polystyrene phantom at 0.5, 0.97, and 1.5 cm from the plane of four  $^{125}\text{I}$  model 6702 seeds in a square array. He found the doses were reduced by 8% if a gold sheet ( $4 \text{ cm} \times 6 \text{ cm} \times 0.3 \text{ mm}$ ) was placed adjacent to the sources in the phantom.<sup>16</sup> Luxton *et al.*, using TLD rods, observed a dose reduction of 4% at 5 mm, 7% at 1 cm, and 10% at 1.8-cm distance from a single 6711 seed, due to the presence of a gold spherical shell ( $18 \times 12 \text{ mm}$  chord length, 1.5 mm thick, radius of curvature 12.5 mm).<sup>17</sup> Wu *et al.*, however, in measurements using TLD cubes at distances of 0.1–1 cm from a single 6711 seed, found the dose to increase when a flat gold shield ( $1.6 \times 2.6 \times 0.1 \text{ cm}$ ) was present.<sup>18</sup> Cygler *et al.*<sup>19</sup> investigated the effect of gold backing ( $110 \times 60 \times 0.1 \text{ mm}$ ) on the dose distribution around an  $^{125}\text{I}$  seed (model 6702) in water using EGS4 Monte Carlo calculation and Diode measurements. They concluded that clinical calculations for  $^{125}\text{I}$  seeds in gold plaque should include a 10% reduction in dose for distances greater than 10 mm and that there is fluorescent x-ray enhancement of dose very close to the source.

Bearing on this issue, we have performed TLD measurements in a solid water eye head phantom with a single 6711 seed at the center of a 20-mm gold plaque of COMS design (with silastic seed carrier insert,  $Z_{\text{eff}}=11$ ). In this paper, we report finding a dose reduction along the plaque central axis (the seed transverse axis) due to the presence of the COMS plaque. The reduction is dependent on distance and approximates 10% at 1 cm. This finding is consistent with our Monte Carlo results (also reported here) for the same plaque configuration. The dose reduction at 17 off-axis TLD measurement points was found to be slightly greater than that along the central axis. When the TLD measurements were repeated to determine the effect of the silastic insert alone (without gold backing), a similar dose reduction pattern was observed.

Further, the effect of the gold backing alone (with natural water replacing the silastic insert) on the  $^{125}\text{I}$  dose distributions was investigated using the MORSE code for plaques of diameters 12 and 20 mm. No significant dose reduction was seen at distances 0.5 cm or less. However, at greater distances, dose reduction was practically the same as for the "silastic alone" configuration. There was no sta-

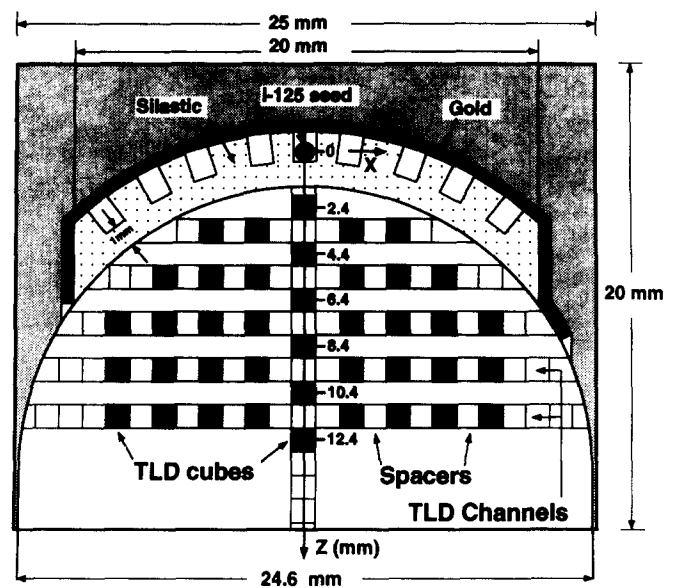


FIG. 1. Cross sectional diagram of eye phantom insert, consisting of three major parts. (1) The eye phantom contains channels accommodating TLD cubes in the phantom central plane. (2) A 20-mm eye plaque of the COMS design, with one  $^{125}\text{I}$  seed at the center slot of the silastic seed carrier insert. (3) A matching piece, designated by the shaded area at the top, maintains the plaque in fixed central position above the eye phantom.

tistically significant difference in the dose reduction pattern for the two different plaque sizes.

## II. MATERIALS AND METHODS

### A. Thermoluminescent dosimetry

We have performed thermoluminescent dosimetry in a solid water<sup>9</sup> eye phantom (Fig. 1) which was embedded in a (solid water) head phantom as shown in Fig. 2. Lithium fluoride TLD-100 cubes (Harshaw Chemical Company), 1 mm on an edge, were used. The TLD protocol for these measurements has been described in an earlier paper.<sup>8</sup> Briefly, it involves tracking the relative sensitivities of individual dosimeters and accounting for fading by comparing responses of TLDs used for measurement with those of control TLDs irradiated (in a Faxitron-type x-ray machine) to a known exposure. Calibration of the control TLD irradiation facility had been performed by comparison with the responses of TLDs irradiated in air at measured distances from  $^{125}\text{I}$  seeds of calibration traceable to the National Institute of Standards and Technology (NIST).

The head phantom's overall dimensions are  $25 \times 25$  cm square and 18.5 cm in height. Sandwiched between the 0.5-cm base plate and the 15-cm stack of slabs, the 3-cm-thick slab had a central cylindrical cavity (2.5 cm in diameter) machined to accommodate the eye phantom insert, as indicated by the shaded region in Fig. 2, and two circular disks (0.5 cm thick each) below the eye phantom insert. The eye-head phantom was supported by styrofoam blocks on two sides resting on the bench top, as shown in

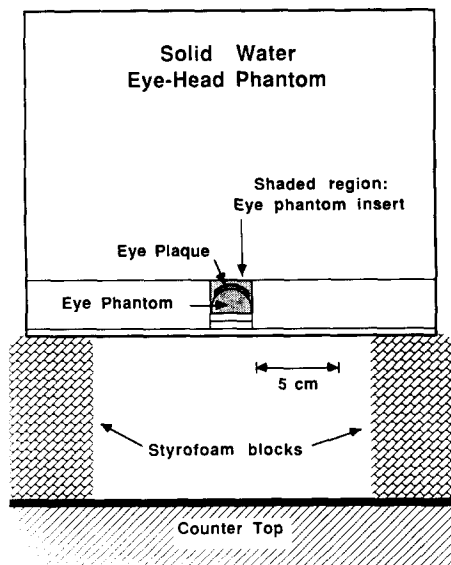


FIG. 2. Diagram of the solid water eye head phantom. The shaded area indicates the eye phantom (see Fig. 1) which, together with two 0.5-cm spacer disks, is inserted in a 3-cm-thick slab that rests on a 0.5-cm base plate.

Fig. 2. The distance from the plaque to the phantom air interface was about 2.5 cm, to simulate eye-head geometry.

The cylindrical eye-phantom insert was made up of three major components: (1) eye phantom, (2) eye plaque, and (3) a matching piece to keep the 20-mm eye plaque in a fixed central position above the eye phantom. The eye phantom insert was 2 cm in height and 2.5 cm in diameter. The eye phantom itself is made of two matching near-quarter-sphere pieces, with the larger quarter containing channels of  $1 \times 1$ -mm-square cross sections to accommodate the TLD cubes and solid water spacers, as shown in Fig. 1. The smaller quarter matches the larger piece to form a near hemisphere, i.e., a hemisphere with a short cylindrical extension. The diameter of the hemisphere was 2.46 cm. The centers of the TLD cubes thus positioned were all in a central plane (A in Fig. 3) of the eye phantom.

A 20-mm eye plaque of the COMS design was applied to the eye phantom for our TLD measurements, as shown in Fig. 1. The gold backing, 0.5 mm thick, consists of a spherical shell segment, and a right circular cylindrical rim (inner diameter 20 mm) terminating the spherical shell segment. The height of the rim was designed to bring it to the outer scleral surface, for which the radius of curvature is taken to be 12.3 mm. The silastic seed-carrier insert is a spherical shell segment which fits snugly into the gold backing. The radius of curvature of the inner concave surface of the insert was designed to be 12.3 mm. Molded into the outer convex surface were seed troughs (or slots) to accommodate the  $^{125}\text{I}$  seeds. The design calls for the closest distance from the concave surface to each trough bottom to be 1 mm. The design thickness of the insert at its center is 2.25 mm. The seed troughs were arranged in ring forms, as shown in Fig. 3. For our TLD measurements, a single  $^{125}\text{I}$

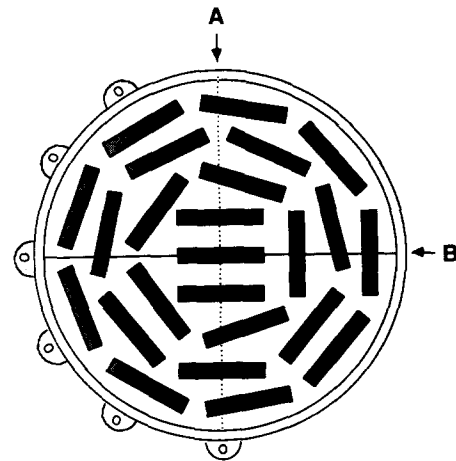


FIG. 3. Diagram of the seed troughs (slots indicated by shaded rectangles) molded into the outer convex curvature of the silastic insert (20 mm in diameter). The central black rectangle represents the seed loading location in our experiments. The dotted line designated by "A" represents the plaque central plane in which the TLD cubes were centered. The solid line indicated by "B" represents the central plane containing the seed longitudinal axis.

seed (model 6711) was situated in the center slot, as indicated by the center black rectangle in Fig. 3. The longitudinal axis of the seed was perpendicular to the eye phantom central plane (A in Fig. 3) that contained the TLD cube centers. The aim was to study the effect of gold and silastic in perturbing the cylindrical symmetry (in a homogeneous medium of the same material) of the  $^{125}\text{I}$  seed dose distribution in this plane.

The eye phantom surface along the central axis ( $z$  axis) was 0.1 cm from the proximal seed surface and hence 0.14 cm from the seed center. The interior scleral surface was taken to be 0.1 cm from the exterior scleral surface and was therefore at 0.24 cm from the seed center. The shaded squares in Fig. 1 indicate the locations of the TLD cubes in the eye phantom. There were six central axis locations, with the TLD cube centers at 0.2-cm intervals beginning at 0.24 cm from the seed center. The off-axis TLD cube locations were arranged in five rows with  $z$  values at 0.2-cm intervals beginning at 0.34 cm. For each experimental run, TLD cubes were loaded in only one "row," including one central axis location and four, six, or eight off-axis locations, depending on the row loaded. Neighboring TLD cubes were always separated by solid-water spacers, to minimize interference effects. The rows not loaded with any TLD cubes in an experimental run were all filled with solid-water spacers to avoid any air cavities between the seed and TLDs.

To study the effect of the silastic insert alone, we repeated the above experiments by leaving out the gold backing. The silastic insert containing the center seed was centered over the eye phantom by the matching piece mentioned earlier.

The exposure time per run ranged from 5 min to 2 h, depending on the distance between the  $^{125}\text{I}$  seed and the TLDs, in order to keep the TLD exposure within the range

TABLE I. Percent-by-weight elemental composition.

	Silastic	Solid water <sup>9</sup>	Natural water
H	6.3	8.09	11.19
C	24.9	67.22	...
N	...	2.4	...
O	28.9	19.84	88.81
Si	39.9	...	...
Cl	...	2.32	...
Ca	...	0.13	...
Pt	0.005	...	...
$\rho$	1.12	1.015	1.0
$Z_{\text{eff}}$	11.2	7.45	7.43

10–40 R. For each gold/silastic combination, up to eight repetitive runs were performed for each TLD loading configuration. The seed strength was calibrated against an NIST-traceable seed of the same model (6711) using a Radiological Physics Center (RPC) well chamber.<sup>20</sup> The seed activity was 24 U (19 mCi) at the beginning and 15 U (12 mCi) at the end of these experiments. The results for symmetric off-axis TLD locations were averaged to yield the data at off-axis points. Dose rates (in  $\text{cGy h}^{-1} \text{U}^{-1}$ ) at central axis and off-axis points were determined, using the TLD calibration factor obtained in our previous study<sup>8</sup> for  $^{125}\text{I}$  seed dose distributions in a homogeneous medium of the same material.

### B. Monte Carlo calculations

Monte Carlo calculations were performed with the seed geometry and plaque configurations incorporated in the combinatorial geometry (CG) module of the MORSE code.<sup>21</sup> The  $^{125}\text{I}$  seed was located at the center of a natural-water sphere 100 cm in radius. The geometric modeling of the seed (model 6711) was identical to that reported in our previous paper.<sup>8</sup> The plaque geometry configurations were modeled after the COMS design<sup>7</sup> as shown in Fig. 1, in order to compare with our TLD measurement data. The gold backing was assumed to be pure gold. For the silastic seed carrier insert (Dow Corning medical grade elastomer, MDX4-4210), the percent-by-weight elemental composition and the physical density used in our calculations were based on information supplied by Dow Corning<sup>22</sup> and are listed in Table I. With nearly 40% silicon by weight, the effective atomic number was estimated to be about 11, substantially higher than that of natural water or solid water.

Four different configurations of plaque geometry were investigated; namely,

- (1) 20-mm diameter, silastic insert, with gold backing;
- (2) 20-mm diameter, silastic insert, without gold backing;
- (3) 20-mm diameter, natural water replacing silastic, with gold backing; and
- (4) 12-mm diameter, natural water replacing silastic, with gold backing.

The Monte Carlo calculation scheme was the same as that used in our previous study.<sup>8</sup> The multigroup cross sections were generated from point cross section data<sup>23</sup> for all the chemical elements involved in the natural water medium and the various heterogeneities. In calculating dose, energy deposition was scored in a cubic region divided into 1000 small cubic bins. The scoring region was situated on the concave side of the plaque, with the bins in one edge row centered on the seed transverse axis (plaque central axis), in order to avoid the need for extrapolation to obtain dose values along the axis. Two sizes of scoring bin were used, namely, 1 and 2 mm on an edge. The sizes of the scoring regions were therefore 1 and 2 cm, respectively, on an edge. For configuration (1), the 1-mm cubic bins were positioned the same way as the TLD cubes in Fig. 1, to enable direct comparison of the TLD data and Monte Carlo results. MORSE code was run until the maximum standard deviation of the mean for any scoring bin was less than 10%. Due to the presence of gold and/or silastic and the resulting absence of cylindrical symmetry around the seed, three-dimensional dose matrices were required. As many as 100 000 000 histories had to be accumulated to achieve acceptable statistics. Russian roulette was used to reduce variance.

Dose values per unit contained activity were obtained. As in our previous paper,<sup>8</sup> the conversion to apparent activity was based on the TLD data for a single 6711 seed in homogeneous medium.

## III. RESULTS

### A. Thermoluminescent dosimetry data

The TLD measurement data are presented as the product of distance-squared and dose rate ( $D$ ) per unit source strength ( $S$ ). Values of  $r^2 D/S$  are plotted vs distance,  $r$ , between the seed center and the TLD cube center, as shown in Fig. 4. The data for the COMS plaque (gold/silastic combination), and for the silastic insert alone (without gold backing), are compared with the TLD data in homogeneous medium of the same material, as reported previously.<sup>8</sup> We noted that the percent dose reduction was *not statistically significantly different* for the two inhomogeneity configurations. (Two-sample  $t$  test<sup>24</sup> was performed for the two sets of data, yielding  $p$  value of 0.88.) The presence of the silastic insert resulted in about 10% dose reduction at 1 cm on the plaque central axis (seed transverse axis) and in larger reductions at greater distances. The addition of the gold backing over the silastic did not further modify the dose distribution within the eye phantom. The average dose reduction at 17 off-axis measurement points was found to be about 15%, slightly greater than that observed for the central axis points.

### B. Monte Carlo results

Dose values in the eye (on the concave side of the plaque) were obtained in three-dimensional matrices using the Monte Carlo method for the four different configurations of plaque geometry mentioned earlier.

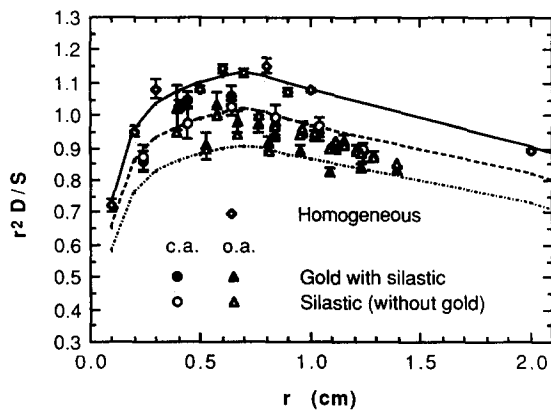


FIG. 4. Results of our TLD measurements for a single  $^{125}\text{I}$  seed (model 6711) in the solid water eye head phantom as shown in Figs. 1 and 2. The values of  $r^2 D/S$  were plotted against distance (between seed center and TLD cube center). The data for gold/silastic combination and silastic alone (without gold backing), shown separately for central axis (c.a.) locations and for off-axis (o.a.) locations of the TLD cubes, are compared with previously reported TLD data<sup>8</sup> for homogeneous medium of the same material.<sup>9</sup> The solid curve indicates the smoothed values for homogeneous medium. The broken and dotted curves represent 90% and 80% of the solid curve values, respectively.

The ratio between (a) dose in natural water with the plaque [either configuration (1), silastic with gold, or configuration (2), silastic alone] in place and (b) dose in natural water<sup>8</sup> with only the  $^{125}\text{I}$  seed present was plotted against distance from seed center along the plaque central axis (see Fig. 5). We noted that the ratios were about 0.9 at points less than 1 cm from the source and were slightly lower at greater distances. Statistical tests<sup>24</sup> were performed to compare the two sets of ratios. The regression analysis  $F$  test yielded a  $p$  value of 0.015. However, because the  $p$  value from a two sample  $t$  test was 0.19, it was inconclusive whether the results were significantly different for configurations (1) and (2).

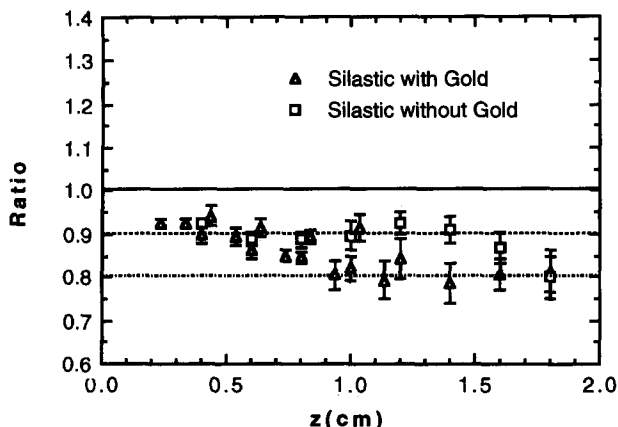


FIG. 5. The ratio of dose involving silastic insert in natural water and dose in homogeneous natural water plotted against distance along plaque central axis, obtained by the Monte Carlo method. The square symbols are for silastic alone without gold backing, configuration (2). The triangular symbols are for gold/silastic combination, configuration (1).

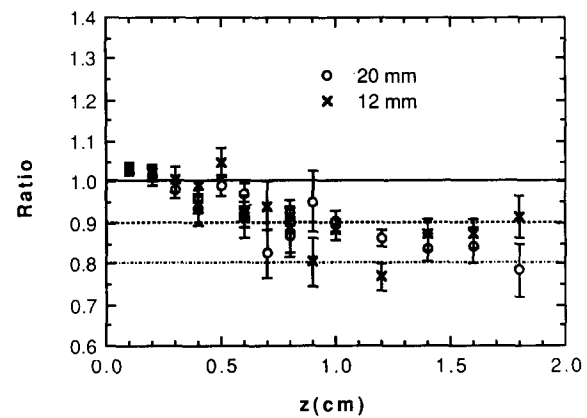


FIG. 6. The ratio of dose involving only gold backing in natural water and dose in homogeneous natural water plotted against distance along plaque central axis. The circle and cross symbols are for gold plaques of diameters, 20 [configuration (3)] and 12 mm [configuration (4)], respectively.

With respect to configurations (3) and (4), the results are shown in Fig. 6. There was *no statistically significant difference* in the dose reduction pattern for the smallest (12 mm) and the largest (20 mm) plaque sizes. (We found  $p$  values of 0.66 from the two-sample  $t$  test and 0.79 from the regression analysis  $F$  test.<sup>24</sup>) No appreciable dose reduction was seen for distances 0.5 cm or closer. However, the dose reduction factor was seen to decrease with increasing distance, approximating 0.9 at 1 cm. These results are generally consistent with data reported, for various forms of plaques, by Weaver,<sup>16</sup> Luxton *et al.*,<sup>17</sup> Wu *et al.*,<sup>18</sup> and Cygler *et al.*<sup>19</sup>

We have also compared Monte Carlo results for configurations (1) and (3) and found the two sets of results to be *statistically significantly different* ( $p$  values of 0.0087 from the two-sample  $t$  test and 0.0074 from the regression analysis  $F$  test<sup>24</sup>). The difference occurs primarily for data at points closer than 1 cm to the source, where the dose for configuration (1), gold plus silastic, appears lower by up to 10% at the closest point (see Figs. 5 and 6).

From the three-dimensional dose matrices obtained by the Monte Carlo calculations for configuration (1) (the gold-silastic combination), we have also generated an isodose plot around the  $^{125}\text{I}$  seed in the plaque central plane (B in Fig. 3). Overall dose reduction of about 10% within the eye was noted along the plaque central axis. Off-axis dose reduction varied from 10%–15% in the eye. Since the scoring region extended up to 2 cm from the seed center, the dose distribution outside the eye was also assessed. The collimating effect of the plaque rim can be seen in Fig. 7, with spatial resolution limited by bin size (1 or 2 mm on an edge) and event statistics.

### C. Comparison of TLD and MORSE results

The TLD data and Monte Carlo results were compared for the gold/silastic combination of the 20-mm COMS design plaque. The ratios of the dose values at 5 central-axis and 17 off-axis locations (see Fig. 1) obtained by these two methods are listed in Table II. Except for two points at

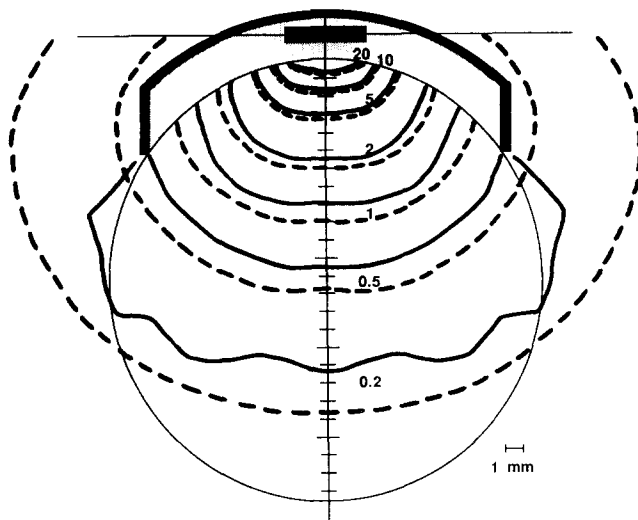


FIG. 7. The solid lines represent the isodose curves in natural water for an  $^{125}\text{I}$  seed (model 6711) at center slot of a 20-mm COMS design plaque in the plaque central plane, indicated by "B" in Fig. 3, obtained by our Monte Carlo calculations. The broken lines are the isodose curves in the same plane for an  $^{125}\text{I}$  seed (model 6711) in homogeneous medium of the same material. The numerals next to the curves indicate the dose rates (in  $\text{cGy h}^{-1}$ ) for a seed with strength of 1.27 U (1 mCi apparent).

extremes of fluctuation in the Monte Carlo data, agreement within about 10% is observed between the two methods.

#### IV. DISCUSSION

The dose values reported here represent the average of the doses within each detector volume. The distance,  $r$ , is the distance between the seed center and the detector center. For the detector locations in the immediate vicinity of the seed (within 0.5 cm), the detector size correction factors may not be negligible. However, the emphasis here is on the relative dose values for the seed in a plaque compared to a homogeneous medium of the same material. Except for second-order effects, the detector size correction factor is cancelled and does not influence the dose ratios.

Other investigators (Wu *et al.*<sup>18</sup> and Cygler *et al.*<sup>19</sup>) have reported that the gold backing enhances the dose in water close to an  $^{125}\text{I}$  seed, an effect attributable to 10-keV

( $L$  shell) fluorescent x rays from the gold. At distances of more than a few millimeters, the dose from fluorescent photons (mean-free-path about 2 mm) is no longer seen, and the remaining effect is one of absorption by gold of scattered  $^{125}\text{I}$  photons. This dose reduction effect (Figs. 4–6) becomes increasingly important as distance increases and the scattered photon dose comprises a larger fraction of the total dose (a circumstance to be expected on the basis of inverse-square attenuation, since the effective distance from the "distributed source" of scattered photons decreases less rapidly than the distance from the seed itself). In the case of the TLD measurements (but not the Monte Carlo calculations), part of the variation in dose reduction may be explained by the greater proximity of the air interface at points farther from the source (see Fig. 2).

Our Monte Carlo results (see Fig. 6) for gold without silastic, in agreement with data reported by others (Wu *et al.*<sup>18</sup> and Cygler *et al.*<sup>19</sup>), show both the near-source enhancement and the reduction at greater distances. In contrast, our results (Fig. 5) with the silastic insert in place show only the dose reduction effect, since, as pointed out by Cygler *et al.*,<sup>19</sup> the fluorescent photons are absorbed in the silastic.

The dose distribution in the peripheral zone of the plaque could not be investigated by TLD measurements with the current design of the eye phantom (Fig. 1). There were small air pockets at the border of this eye phantom during the experimental setup. In addition, the noncentral troughs in the seed carrier insert were left empty, hence leaving 23 air pockets in the insert. The effect of these above-mentioned air pockets needs to be resolved. A new eye phantom design for a future study of dose distributions inside and outside the eye is under way. The air pockets near the eye border would be eliminated in the new design. The troughs not occupied by the active seed would be filled with "spent" seeds to study the effect of the silver and titanium inhomogeneity in the surrounding seeds. In addition, we are going to use smaller TLD detectors ( $1 \times 1 \times 0.5$  mm) in the future measurements to reduce detector volume effect.

Using the Monte Carlo method, a plaque collimating effect can be seen at the periphery (see Fig. 7). However, the currently used bin sizes (1- or 2-mm cubes) are not small enough to yield adequate penumbra information at spatial resolution finer than 1 mm. Reducing the scoring bin size would improve the spatial resolution, but would require more computer time.

The lip-collimating effect of the plaque depends on the location of the seed in the insert. It is planned to carry out further measurements and calculations for various seed locations, in order to provide reference data for a more accurate evaluation of doses delivered.

The differences noted in Table II may in part be related to differences between the solid water used for our TLD measurements and the natural water assumed in our Monte Carlo calculations. Williamson<sup>25</sup> has reported the results of Monte Carlo calculations for  $^{125}\text{I}$  sources; he found the dose rate constant in solid water to be 4.3% less than that in natural water. The difference was more pro-

TABLE II. The ratios of the dose values obtained by Monte Carlo and TLD methods at central-axis ( $x=0$ ) and off-axis locations for 20-mm COMS plaque.

$x(\text{cm})$	0	0.2	0.4	0.6	0.8
$z(\text{cm})$					
0.24	$1.08 \pm 4\%$	...	...	...	...
0.34	...	$0.91 \pm 6\%$	$0.99 \pm 4\%$	...	...
0.44	$0.99 \pm 3\%$	...	...	...	...
0.54	...	$0.96 \pm 4\%$	$0.96 \pm 4\%$	$0.94 \pm 3\%$	...
0.64	$0.96 \pm 4\%$	...	...	...	...
0.74	...	$0.97 \pm 3\%$	$0.93 \pm 4\%$	$1.00 \pm 4\%$	$0.97 \pm 4\%$
0.84	$1.01 \pm 3\%$	...	...	...	...
0.94	...	$0.95 \pm 4\%$	$0.81 \pm 4\%$	$0.96 \pm 5\%$	$0.91 \pm 3\%$
1.04	$1.04 \pm 4\%$	...	...	...	...
1.14	...	$0.92 \pm 4\%$	$0.90 \pm 5\%$	$0.91 \pm 6\%$	$0.81 \pm 8\%$

nounced with increasing distance from the source and reached 8% at 3 cm.

## V. CONCLUSIONS

We have investigated the dose reduction effect for an  $^{125}\text{I}$  seed (model 6711) due to the presence of gold and/or silastic in an eye plaque. The dose reduction was found to depend on the distance and off-axis locations. The effect of the silastic insert alone was found to be closely the same as the silastic/gold combination. The reduction was about 10% at 1 cm, with reduction of the order of 15% at 2 cm and at off-axis points.

## ACKNOWLEDGMENTS

One of the authors (STCT) would like to thank Dr. Chen-Shou Chui for helpful discussions regarding appropriate input parameters for eye plaque geometry in using the combinatorial geometry module of the MORSE code, as well as Mr. David Kubiawicz (3M Company) for supplying dimensional and material data on the Model 6711  $^{125}\text{I}$  seed. The extensive help by Dr. Yu Li in TLD data acquisition and reduction is also gratefully acknowledged. This work was supported in part by NCI Contract No. NO1-CM-57776 and NEI Grant No. RO1-EY08131.

<sup>1</sup>M. Rotman, S. Packer, R. Long, S. Chiu-Tsao, and L. Z. Sedhom, "Ophthalmic plaque irradiation of choroidal melanoma," in P. K. Lommatzsch and F. C. Blodi, *Intraocular tumors* (Springer, Berlin, 1983), pp. 341-346.

<sup>2</sup>S. Packer, M. Rotman, R. G. Fairchild, D. M. Albert, H. L. Atkins, and B. Chan, "Irradiation of choroidal melanoma with iodine 125 ophthalmic plaque," *Arch. Ophthalmol.* **98**, 1453-1457 (1980).

<sup>3</sup>S. Packer, M. Rotman, and P. Salanitro, "Iodine-125 irradiation of choroidal melanoma, clinical experience," *Ophthalmology* **91**, 1700-1708 (1984).

<sup>4</sup>K. Weaver, R. Peksens, and C. Barnett, "Special brachytherapy procedures and dosimetry for tumors of the brain, eye, head and neck, and perineum," in J. G. Kereiakes, H. R. Elson, and C. G. Born, *Radiation oncology physics 1986*, Medical Physics Monograph No. 15 (American Institute of Physics, New York, 1987), pp. 677-699.

<sup>5</sup>S. Chiu-Tsao, K. O'Brien, R. Sanna, H. S. Tsao, C. Vialotti, Y. S. Chang, M. Rotman, and S. Packer, "Monte Carlo dosimetry for  $^{125}\text{I}$  and  $^{60}\text{Co}$  in eye plaque therapy," *Med. Phys.* **13**, 678-682 (1986).

<sup>6</sup>J. Earle, R. W. Kline, and D. M. Robertson, "Selection of iodine-125 for the collaborative ocular melanoma study," *Arch. Ophthalmol.* **105**, 763-764 (1987).

<sup>7</sup>R. W. Kline and P. D. Yeakel, "Ocular melanoma, I-125 plaques," *Med. Phys.* **14**, 475 (1987).

<sup>8</sup>S. Chiu-Tsao, L. L. Anderson, K. O'Brien, and R. Sanna, "Dose rate determination for  $^{125}\text{I}$  seeds," *Med. Phys.* **17**, 815-825 (1990).

<sup>9</sup>C. Constantinou, F. H. Attix, and B. R. Paliwal, "A solid water phantom for radiotherapy x-ray and  $\gamma$ -ray beam calibrations," *Med. Phys.* **9**, 436-440 (1982).

<sup>10</sup>J. F. Williamson, "Theoretical evaluation of dose distributions in water about models 6711 and 6702  $^{125}\text{I}$  seeds," *Med. Phys.* **15**, 891-897 (1988).

<sup>11</sup>C. C. Ling, E. D. Yorke, I. J. Spiro, D. Kubiawicz, and D. Bennett, "Physical dosimetry of  $^{125}\text{I}$  seeds of a new design for interstitial implant," *Int. J. Radiation Oncol. Biol. Phys.* **9**, 1747-1752 (1983).

<sup>12</sup>J. F. Williamson and R. Nath, "Clinical implementation of AAPM Task Group 32 recommendations on brachytherapy source strength specification," *Med Phys.* **18**, 439-448 (1991).

<sup>13</sup>L. L. Anderson, R. Nath, K. A. Weaver, D. Nori, T. L. Phillips, Y. H. Son, S. Chiu-Tsao, A. S. Meigooni, J. A. Meli, and V. Smith, *Interstitial Brachytherapy, Physical, Biological and Clinical Considerations*, (Raven Press, New York, 1990).

<sup>14</sup>K. A. Weaver, V. Smith, D. Huang, C. Barnett, M. Schell, and C. Ling, "Dose parameters of  $^{125}\text{I}$  and  $^{192}\text{Ir}$  seed sources," *Med. Phys.* **18**, 636-643 (1989).

<sup>15</sup>R. Nath, A. S. Meigooni, and J. A. Meli, "Dosimetry on transverse axes of  $^{125}\text{I}$  and  $^{192}\text{Ir}$  interstitial brachytherapy sources," *Med. Phys.* **17**, 1032-1040 (1990).

<sup>16</sup>K. A. Weaver, "The dosimetry of  $^{125}\text{I}$  seed eye plaques," *Med. Phys.* **13**, 78-83 (1986).

<sup>17</sup>G. Luxton, M. A. Astrahan, and Z. Petrovich, "Backscatter measurements from a single seed of  $^{125}\text{I}$  for ophthalmic plaque dosimetry," *Med. Phys.* **15**, 397-400 (1988).

<sup>18</sup>A. Wu, E. S. Sternick, and D. J. Muise, "Effect of gold shielding on the dosimetry of an I-125 seed at close range," *Med. Phys.* **15**, 627-628 (1988).

<sup>19</sup>J. Cygler, J. Szanto, M. Soubra, and D. Rogers, "Effects of gold and silver backings on the dose rate around an  $^{125}\text{I}$  seed," *Med. Phys.* **17**, 172-178 (1990).

<sup>20</sup>L. W. Berkley, W. F. Hanson, and R. J. Shalek, "Discussion of the characteristics and results of measurements with a portable well ionization chamber for calibration of brachytherapy sources," in D. Shearer, *Recent advances in brachytherapy physics*, Medical Physics Monograph 7 (American Institute of Physics, New York, 1981).

<sup>21</sup>MORSE-CG, General purpose Monte Carlo multigroup neutron and gamma-ray transport code with combinatorial geometry, ORNL, Radiation Shielding Information Center Computer Code Collection, CCC-203.

<sup>22</sup>M. Musolf, Dow Corning Medical Group, personal communication.

<sup>23</sup>E. F. Plechaty, D. E. Cullen, and R. J. Howerton, Tables and graphs of photon-interaction cross sections from 0.1 keV to 100 MeV Derived from the LLL Evaluated Nuclear Data Library, LLL, UCRL-50400, Vol. 6, Rev. 3, Distribution Category UC-34, 1981.

<sup>24</sup>B. Ryan, B. Joiner, and T. Ryan, Jr., *Minitab\* Handbook* (Duxbury, MA, 1985), pp. 95-99, 185-192, 223-235. (Minitab is a registered trademark of Minitab, Inc., and it is the statistical software package used for our analysis.)

<sup>25</sup>J. F. Williamson, "Comparison of measured and calculated dose rates in water near I-125 and Ir-192 seeds," *Med. Phys.* **18**, 776-786 (1991).